Manuscript version
DOI original paper: 10.1115/DETC2020-22383

Real-time applicable power management of multi-source fuel cell vehicles using situation-based model predictive control

Ahmed M. Ali[1,*], Dirk Söffker[1,]

Chair of Dynamics and Control, University of Duisburg-Essen, Lotharstr. 1, 47057 Duisburg, Germany

Abstract

Power management in all-electric powertrains has a significant potential to optimally handle the limited capability of electric power sources and to promote electromobility towards competitive performance levels. Real-time applicability of optimization-based power management strategies (PMSs) is an open challenge, leading to increasing attention in recent literature. Situation-based PMSs (SB-PMSs), defining optimized solutions related to specific vehicle situations, offer the ability to reduce computational requirements and enhance the optimality of simple rule-based algorithms. However, the achievable optimality in such PMSs is limited to local optimality in each situation. This degraded, yet improvable, optimality in SB-PMSs can be addressed by considering online optimization of the situated solutions for limited horizons to approach the global optimal solution. In this context, model predictive control is an efficient optimization method that suits real-time application. However, the availability of valid plant model and a priori prediction of upcoming driving conditions are prerequisites for MPC. Finding suitable solutions to these challenges in PMSs contributes to better control of hybrid electric vehicles. This papers presents a novel PMSs that implements situation-based MPC to define optimal control strategies for fuel cell hybrid vehicles. Vehicle states are defined in terms of multiple characteristic variables and power management decisions are optimized offline for each vehicle states. Prediction of vehicle states is performed using statistical predictive model based on state transitions in a number of driving cycles. Pre-optimized solutions related to predicted states are iterated online to achieve better optimality for the look-ahead horizon. Results analysis from online testing revealed the ability of SB-MPC to reduce total energy cost in different driving cycles.

Keywords: Fuel cell HEVs, model predictive control, power management, real-time optimization

1. Introduction

1.1. Background and motivation

Increasing concerns about pollutant emissions and depletion of limited fossil fuel reserves motivated the pursuit towards alternative clean transportation systems [1]. In the last few years, all-electric vehicles (AEVs) proved competitive performance levels compared to their counterparts, combustion engine-based vehicles, at significantly reduced emissions [2, 3]. Moreover, the accelerating advances in fuel cell, battery, and supercapacitors' technologies fastened the pace towards further hybridization paradigms offering more flexible power handling [4]. Therefore, such electrified powertrains have moved progressively from being short-term alternatives towards being a promising state-of-the-art that receives increasing attention from both researchers and automakers [5].

Power management strategies (PMSs) in hybrid powertrains promote efficient operation of multiple power sources without mitigating vehicle's driveability. It is required from an efficient PMS to accommodate unscheduled loads and achieve maximum overall efficiency at different power split paradigms of the vehicle [6]. Existing power management algorithms can be categorized into rule-based and optimization-based ones. In rule-based algorithms, the control law is formulated using heuristics and practical experience. Lack of solution optimality is a major disadvantage of rule-based PMSs; however, such algorithms are widely applied due to their simple implementation. Contrarily, optimization-based algorithms are formulated to achieve global optimal solutions in certain driving scenarios [7]. The obtained optimal solutions are rather related to specific driving cycle for optimization and hence can be used as a benchmark solution for evaluation purposes [8].

To overcome the drawbacks in both categories and achieve better optimality in real-time, many innovative attempts have been made to define optimized situation-based solutions to power management problem [9]. These solutions can be applied online according to the recognized situation, achieving near optimal solutions at significantly reduced computational load [10]. In this context, the definition of vehicle states in terms of multiple characteristic variables (in situation-based PMS) received further attention to develop situated prediction models [11]. Such prediction models can be integrated to online optimization algorithms such as model predictive control (MPC), which has been widely and efficiently applied to opti-

*Corresponding author
Email addresses: ahmed.ali@uni-due.de (Ahmed M. Ali), soeffker@uni-due.de (Dirk Söffker)
[1]All the authors have equally contributed to the manuscript.

mal power management of hybrid powertrains [12].

Resolving the conflict between solutions' optimality, robustness, and computational load of optimization-based PMSs an important aspect that contributes to the real-time applicability of developed methods [13, 12]. Defining intelligent situation-based solutions to online PMSs offers better solutions' optimality and less computational requirements [9]. For online optimization, MPC can significantly contribute to optimal control decisions in real-time due to its ability to handle complex constraints of the power management problem. A brief survey on the achievements in situation-based PMSs and MPC in hybrid electric powertrains is given in the sequel, putting forth the recent challenges and potential development aspects.

1.2. Previous work

1.2.1. Situation-based PM methods

The principle of a situation-based PMS (SB-PMS) is based on implementing two main control layers to define power split decisions: an online and offline one as shown in Fig. 1. Vehicle states are typically defined in terms of characteristic variables, i.a. the driver's power demand, vehicle operating conditions, and other external information (traffic, road grade, altitude, etc) [14]. Theses information are used to generate database for the offline layer, in which discrete vehicle states can be defined [15]. Optimal combination of these variables at respective discretization levels is of particular importance in SB-PMS and is separately discussed in the sequel. For defined vehicle states, power handling strategies can be optimized offline. Driving information from the database are used to provide the characteristics of driving cycles' segments related to each vehicle state (vehicle speed, power demand, distance, ...etc.). Such solutions are be integrated to the online layer in LUTs' form, to be applied when according vehicle states are recognized. This operating scheme offers the advantage of decoupling computational loads of the optimization process from online control layer and hence the ability to achieve near optimal solutions in real-time [11, 16].

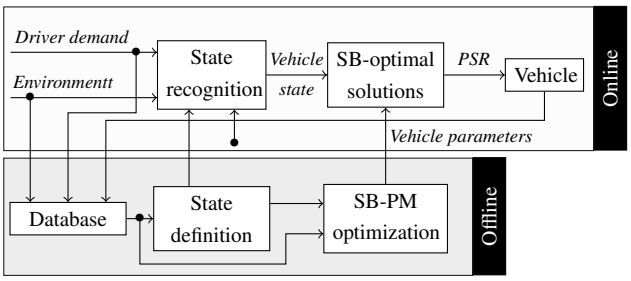

Figure 1: Operating principle of situation-based power management system (SB-PMS), defining optimal power split ratios (PSR) for vehicle states in real-time.

The selection of characteristic variables to define vehicle states is a crucial point in SB-PMSs, that influences its ability to recognize such states online and the potential of finding suitable optimal solutions offline. A brief survey on pattern recognition attempts for power management strategies gives the conclusion

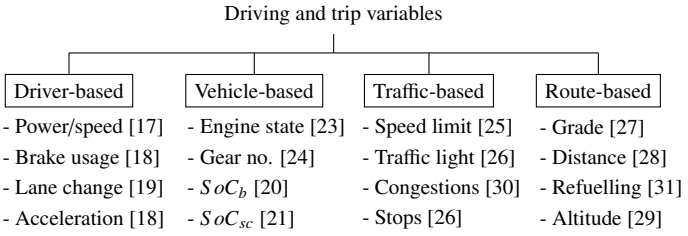

Figure 2: Classification of driving- and trip variables according to their dependency reference.

that characteristic parameters can be related to variables from four categories: driver-, traffic-, vehicle-, and route-based ones as illustrated in Fig. 2 [11]. Power demand and vehicle speed are implemented most frequently in SB-PMSs due to their direct impact on power handling constraints [17, 18]. Information about vehicle speed and power demand, combined with accelerating behavior, lane change, and braking usage provide essential knowledge of individual driving behaviors, which enables determining specific power handling rules to avoid excessive energy consumption due to abrupt or aggressive driving [18, 19].

Characteristic parameters related to battery's or supercapacitor's state of charge (SoC_b, SoC_{sc}) are widely implemented to represent on-board energy reserve in vehicle state definition [20, 21, 22]. Other variables with discrete values, i.e. (gear numbers or engine status), are typically used in dynamic programming to define state space of possible power handling strategies for specific trips [23, 24]. The accelerating advances in telematics offer useful information about speed limits and traffic lights [25, 26]. Besides, in case of pre-known driven routes, further information about road grade and trip distance can be acquired [27, 28, 29]. Suck knowledge enables the PMS to determine suitable strategies to avoid idling losses during traffic congestion or repetitive stops [30, 26]. Moreover, specific regulations of power handling can be put forth targeting low-cost power grids for recharging [31].

A significant application of multi-parametric definition of vehicle situations is the development of state prediction models [11, 32]. Typically, artificial neural networks, machine learning, or hidden Markov models are used to evaluate the impact of different characteristic variables on the prediction accuracy of vehicle situation [33]. Such prediction models can be used online to define optimal power management strategies for upcoming predicted horizon. However, the assessment between offline optimized solutions, prediction accuracy, and online applicability using certain constellations of characteristic variables is not yet introduced in literature.

1.2.2. Model predictive control in HEVs

Model predictive control is an online optimization-based method, that proved applicability in many fields, i.a. power management of hybrid electric vehicles [12]. Attractive features of MPC include the ability to perform in real-time and to to handle complex constraints on inputs, outputs, and system

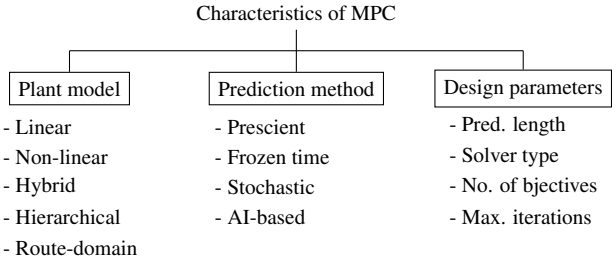

Figure 3: Summary of MPC characteristics considering modeling, design, and prediction methods [12].

states to operate hybrid powertrains closer to system boundaries, which increases the optimality of provided solutions [34, 12, 35]. Therefore, targeting solution's optimality for an extended time-horizon, MPC outperforms instantaneous optimization methods, i.a. equivalent cost minimization (ECMS) [36]. Given an accurate prediction of upcoming driving conditions, MPC proved the ability to achieve 96 % of the global optimality obtained by full-DP [37].

For MPC-based PMSs, a prediction of vehicle state is required beforehand, to which optimal control strategy can be iteratively searched [38, 39]. This prediction can be performed using different approaches, i.a. stochastic models [40, 41], neural networks [42], fuzzy logic, [43], or by considering particular prescient assumption [37]. System response to proposed control strategies can be anticipated using plant model. Such model can be linear, non-linear, or hybrid models [44, 45, 46]. State prediction outside time-domain has been also introduced based on route information only [47]. Other design parameters of MPC are the length of prediction horizon, number of objectives in the cost function, solver type, and number of iterations per time step to meet the optimality criterion [12]. These characteristic of MPC are summarized in Fig. 3.

Considering pre-optimized situation-based solutions in MPC can significantly reduce the computational time to meet defined optimality criteria [48, 49]. This offers the advantage of considering longer look-ahead horizons for optimization and hence yield near-global optimal solutions [42, 50]. However, very few attempts to realize this concept for PMSs of HEVs can be found in literature [12].

1.3. Problem statement, contribution, and novelty

The introduced review about SB-PMSs and MPC in HEVs gives an insight into the significance of both approaches to realize optimal power management decisions in real-time. However, following aspects is less addressed in literature: First, although selection of the characteristic variables and their respective discretization has a significant impact on optimization results in SB-PMSs, this aspect is not considered so far for optimization. Second, the integration of such multi-parametric state-definition in the formulation of optimal control problem in MPC-based PMSs has not been realized.These two aspects have a significant potential to improve the applicability of MPC-based PMSs in HEVs through precise definition of vehicle states and the ability to sustain near-optimal solutions in real-time.

This contribution proposes a novel SB-PMS that implements MPC to define optimal control strategies for fuel cell electric vehicles. Vehicle states in each situation are optimally defined in terms of multiple characteristic variables. Offline-optimization of control decisions for each vehicle state is performed using NSGA-II. The optimized solutions are online-control as look-up tables. Optimal power management strategies for upcoming vehicle states are iterated online based the tabulated solutions using MPC. A state prediction model is developed based on the selected characteristic variables using Markov process. The introduced method is adapted to suit real-time application in terms of maximum look-ahead size and number of iteration per time step. Online testing using several driving cycles is carried out to comparatively evaluate the developed PMS.

This paper is organized as follows: Vehicle model and supervisory control are introduced in section 2. Problem formulation in SB-PMS and MPC is explained in section 3. Online application and results analysis are given in section 4. Finally, conclusion and future work are presented in section 5.

2. Powertrain description

The implemented powertrain in this study is a hybrid all-electric one, that comprises a fuel cell, battery, and supercapacitor (Fig. 4). These power sources are set up in a series-parallel topology, whereby the fuel cell is the primary power source and both the battery and supercapacitor are auxiliary ones. Each power source is coupled with an inline DC/DC converter, sustaining a unified voltage u_{bus} at the load side. This drive-line topology is investigated to achieve an optimal performance for fuel cell hybrid powertrains [51].

The power demand p_d is calculated within using the vehicle model as

$$\begin{aligned} p_d &= f_x v \\ &= \left(ma + \underbrace{\frac{A\rho C_d}{2}(v - v_d)^2}_{\text{Air drag}} + \underbrace{mg\sin\theta}_{\text{Grade res.}} + \underbrace{\mu mg\cos\theta}_{\text{Rolling res.}} \right) v, \end{aligned} \quad (1)$$

where f_x denotes traction force, mg vehicle curb weight, a longitudinal acceleration, ρ air density, A vehicle frontal area, C_d air drag coefficient, v_d wind speed, μ rolling resistance coefficient, and θ the road grade. The power management system (PMS) in Fig. 4 consists of two sub-modules: supervisory control and the situation-based MPC (SB-MPC). The latter module is responsible of finding optimal power handling strategies in real-time, to which a brief explanation is given in section 3. The main task of the supervisory control module is to count for the operating limits of individual powertrain components and therefore override erroneous power handling strategies in case of on-board charge depletion.

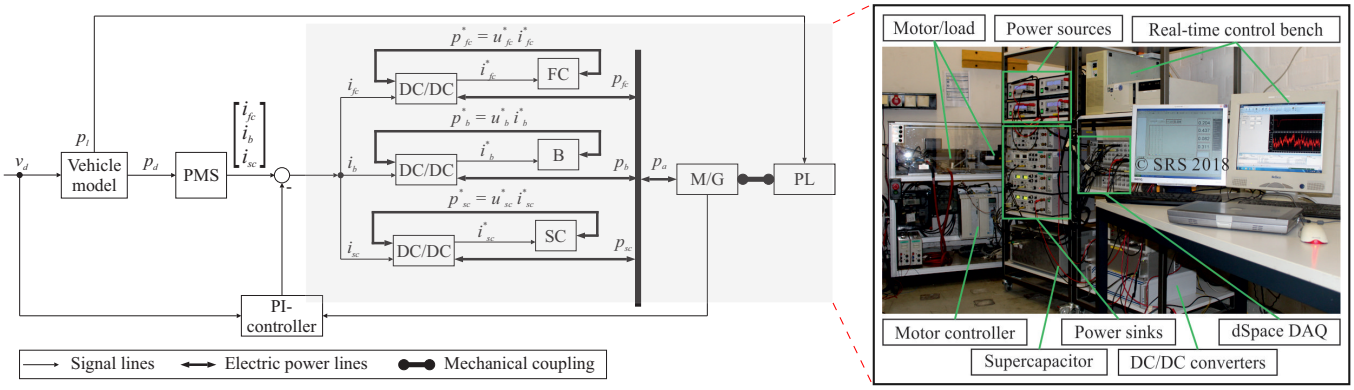

Figure 4: Vehicle model and integrated HIL emulation test-rig of the multi-source electric powertrain (Chair of Dynamics and Control, University of Duisburg-Essen, Germany).

The power demand from each source p_{fc}, p_b, and p_{sc} is defined as

$$p_{fc} = u_{fc}\, i_{fc}, \tag{2}$$
$$p_b = u_b\, i_b, \text{and} \tag{3}$$
$$p_{sc} = u_{sc}\, i_{sc}, \tag{4}$$

where the bus voltage u_{bus} is equalized through the inline DC/DC converters as

$$u_{fc} \approx u_b \approx u_{sc} \approx u_{bus}, \tag{5}$$

implying that only desired output current from each source can be used as control signal to respective DC/DC converter as $[i_{fc}\ i_b\ isc]^T$. The operation of DC/DC converter can be simplified as

$$i_{in} = i_{out}\, \frac{c}{u_{in}}\, \frac{1}{\mu_{conv}}, \tag{6}$$

where the subscripts $_{in}$ and $_{out}$ denote input and output voltage/current values, c is a constant representing desired bus voltage, and μ_{conv} is the tabulated conversion efficiency based on experimental validation of the simplified model [51]. The output i_{out} of each DC/DC converter represents the control signals i^*_{fc}, i^*_b, and i^*_{sc} for the fuel cell, the battery, and the supercapacitor accordingly. The fuel cell voltage is calculated considering activation-, ohmic-, and concentration-voltage losses as

$$\begin{aligned} u^*_{fc} = n_c(u^o_{fc} &- \underbrace{\left(c_1 + c_2\left(1 - e^{-i^*_{fc} c_3}\right)\right)}_{u_{act}} \ldots \\ &- \underbrace{i^*_{fc}\, R_{fc}}_{u_{ohm}} \ldots \\ &- \underbrace{i^*_{fc}\left(\frac{c_4\, i^*_{fc}}{i_{max}}\right)^{c_5}}_{u_{conc}}), \end{aligned} \tag{7}$$

where n_c denotes the number of cell in the stack, u^o_{fc} the open circuit voltage, $c_1, ..., c_5$ constants based on experimental validation, R_{fc} the internal resistance of the fuel cell, and i_{max} the maximum delivery current. The battery is modeled based on the equivalent RC circuit as

$$u^*_b = u^o_b - R_b\, i^*_b - \frac{1}{C_b}\int_{t_i}^{t_f} i^*_b\, dt, \tag{8}$$

where u^o_b is the open circuit voltage, R_b and C_b are battery's capacitance and internal resistance accordingly, and t_i and t_f are initial and final time of an infinitesimal simulation step. Similarly, the supercapacitor is modeled as

$$u^*_{sc} = u^o_{sc} - R_{sc}\, i^*_{sc} - \frac{1}{c_{sc}}\int_{t_i}^{t_f} i^*_{sc}\, dt, \tag{9}$$

where u^o_{sc} is the open circuit voltage, R_{sc} and C_{sc} are equivalent capacitance and internal resistance of the supercapacitor accordingly. Both C_b and C_{sc} are statically modeled neglecting the capacitance loss due to components' aging and lifetime degradation. The state of charge of (SoC) for either sources is calculated as

$$SoC = SoC_i - \frac{1}{Q_{nom}}\int_{t_i}^{t_f} I\, dt, \tag{10}$$

where SoC_i is the initial state of charge, Q_{nom} the rated capacity, and I is either respective current (i_b or i_{sc}). The actual power delivery p_a at motor terminals is calculated considering conversion losses as

$$\begin{aligned} p_a &= p_{fc} + p_b + p_{sc} \\ &= p^*_{fc} + p^*_b + p^*_{sc} + losses. \end{aligned} \tag{11}$$

so that p_{fc}, p_b, and p_{sc} are determined based on the split ratio $\psi = [\beta \quad \gamma]$ as

$$\begin{bmatrix} p_{fc} & p_b & p_{sc} \end{bmatrix}^T = \begin{bmatrix} \beta & \gamma & 1-(\beta+\gamma) \end{bmatrix}^T p_d, \tag{12}$$

subjects to driveability constraint

$$\beta + \gamma \leqslant 1, \quad \forall\ \{\beta, \gamma\} \in [0, 1]. \tag{13}$$

For the emulation test-rig, the traction motor is mechanically coupled to a programmable load-motor emulating the rolling resistance, road grade, and air drag according to the speed input v and driving cycle information [51].

3. Situation-based model predictive control

3.1. Vehicle state definition

This contribution is focused to the implementation of MPC-based power management based on the corporate definition for vehicle states; in terms of multiple characteristic variables. Vehicle states are linearly mapped into a multi-dimensional space, referred to as grid-space (GS), where selected variables (vehicle speed, power demand, ... etc.) can be depicted as axes. The number of variables considered for state definition and their respective discretization levels are two main aspects determining the ability of GS constellation to meet following objectives: first, defining vehicle states, to which power handling decisions can be optimized offline (see Fig. 1) Second, providing reusable transition statistics between states to develop state prediction models; which is a prerequisite to online optimization using MPC. These aspects have been investigated in previous work of the authors [52]. Relevant findings from [52] are briefly explained as required in the sequel.

The characteristic variables for state definition are related to vehicle speed v, power demand p_d, and on-board states of charge SoC_b and SoC_{sc}. Speed dynamics is also implemented considering speed fluctuation (frequency), magnitude, and acceleration to represent driver's behavior in receding time horizon. The vectors comprising discrete levels for the characteristic variables are V, P, B, and SC, and D respectively. To exemplify how optimal values for the discrete levels are determined, discrete levels for V can be defined as

$$V^n = [V_1, V_2, ..., V_n], \tag{14}$$

where n denotes the total number of discrete levels and is set arbitrarily for each variable.

Numerical values for each discrete level are optimized to achieve better representation of vehicle states in GS, i.e. less number of missed states and maximum homogeneity of points count. Driving history from 24 driving cycles (Fig. 5c), is used to carry out the optimization task

$$\text{minimize} \quad \mathrm{J}_1 = f(\mathrm{N}_v, V^n), \tag{15a}$$

s.t.

$$\mathrm{V}^n(i) \in [v_{min} \;\; v_{max}], \tag{15b}$$

where N_v denotes all sample points of v in database. The throughput of f is the difference in points' count between the intervals from $[V_i^n : V_{i+1}^n]$, for $i = 1, 2, ..., n$. This optimization task is solved offline using NSGA-II based on the work of [53, 54]. The achievement of this step is shown in Fig. 5 for both equally- and optimally-discretized GS-axes.

Based on the above-explained aspects, a total of 162 different constellations for GS have been generated considering multiple combinations of GS-axes and different discrete levels for each variable. The total number of states in each constellation of GS is related to its respective combination of axes as shown in Fig. 6. The axes configuration for constellation C3 is shown also in the figure defining, illustrating how two arbitrary states s_{12} and s_{38} out of total number of 60 states are defined [52].

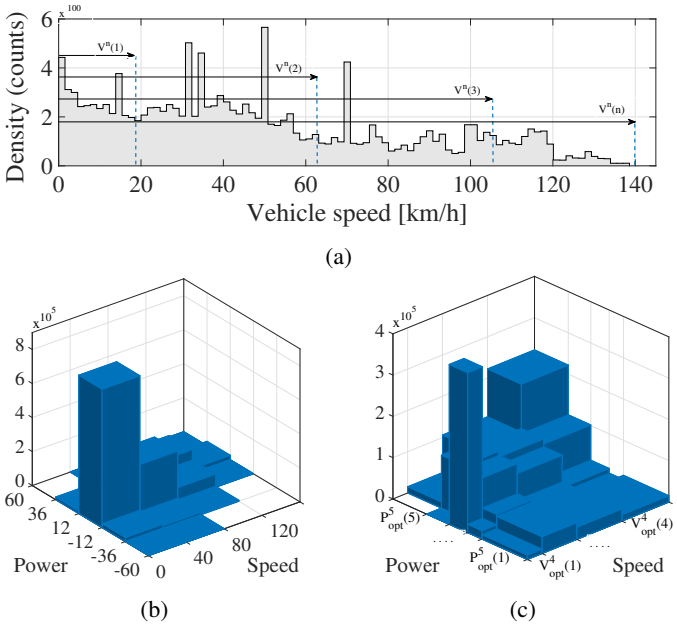

Figure 5: Optimal discretization of GS-axes: Defining points count for each variable in gathered database (5a). Improving vehicle states representation in GS using optimally-spaced axes in (5c) compared to equally-spaced ones in (5b).

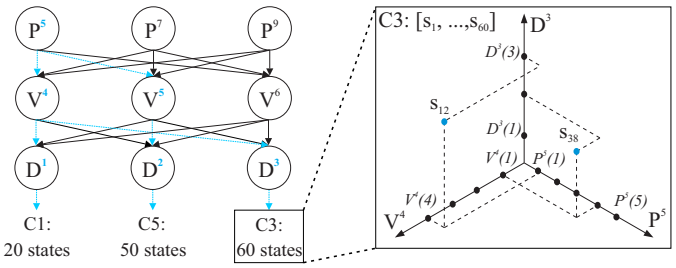

Figure 6: Implementation of characteristic variables in grid-space structure with focus on state definition in an exemplified constellations C3.

Optimal power split for each state in GS is searched. The control vector to be optimized is

$$\Psi = [\psi_1 \quad \psi_2 \quad ... \quad \psi_m], \tag{16}$$

where ψ_i denotes split ratio associated to respective vehicle state $s_i \; \forall \; i \in \{1, 2, ..., m\}$. The optimization task is defined as

$$\min \quad J = \min \begin{bmatrix} obj_1(u, x, t) \\ obj_2(u, x, t) \end{bmatrix}, \tag{17}$$

for

$$obj_1(u, x, t) = \int_{\tau}^{\tau+T} m_{eq} \, d\tau \qquad \text{and} \tag{18}$$

$$obj_2(u, x, t) = \alpha_1 \, \Delta SoC_b \, |_{t=\tau}^{t=\tau+T} + \alpha_2 \, \Delta SoC_{sc} \, |_{t=\tau}^{t=\tau+T}, \tag{19}$$

s.t.

$$SoC_b^{min} < SoC_b < SoC_b^{max}, \tag{20a}$$
$$SoC_b^{min} < SoC_b < SoC_b^{max}, \tag{20b}$$
$$p_{fc}^{min} < p_{fc} < p_{fc}^{max}, \tag{20c}$$
$$p_b^{min} < p_b < p_b^{max}, \tag{20d}$$
$$p_{sc}^{min} < p_{sc} < p_{sc}^{max}, \text{and} \tag{20e}$$
$$\beta + \gamma \leqslant 1, \qquad \forall \ \{\beta, \gamma\} \in [0,1], \tag{20f}$$

where the superscripts ^{min} and ^{max} denote minimum and maximum limits for related variables and m_{eq} the function calculating equivalent fuel consumption of the fuel cell considering the conversion ratio (33.7 kWh/GGE), according to [51]. Values for weighting factors α_1 and α_2 are considered as 60 and 40 % respectively to utilize the relative capability of battery and supercapacitor to take over dynamic power demand through fast recharging/discharging better than the fuel cell. The optimized solution vector $u = [\Psi]$ is integrated to the online application using MPC.

3.2. State prediction model

State prediction models are prerequisite for real-time optimization-based PMS. Accurate definition of vehicle states in GS offers the ability to associate offline-optimized solution to certain operating conditions and hence significantly narrow down the online iteration process. Therefore, it is essential to determine GS constellation, in which transitions between vehicle states can be implemented to develop accurate prediction models. In such models, vehicle state at a time instant k can be defined as

$$S_k \in \{s_1, s_2, ..., s_m\}, \tag{21}$$

where m is the total number of states in each constellation (see Fig. 6). Markov property for an order-one chain can be defined for the stochastic process χ as

$$\begin{aligned} &Pr\left(\chi_{k+1} = S_{k+1} \mid \chi_k = S_k, \chi_{k-1} = S_{k-1}, ..., \chi_1 = S_1\right) \\ &\quad = Pr\left(\chi_{k+1} = S_{k+1} \mid \chi_k = S_k, \chi_{k-1} = S_{k-1}\right). \end{aligned} \tag{22}$$

The transition probability Γ_{ij}^h to a next state $S_{k+1} = s_j$, in case of having previous and current states as $S_{k-1} = s_h$ and $S_k = s_i$ respectively can be calculated using driving database to obtain the transition probability matrix

$$\Gamma^h = \begin{bmatrix} \Gamma_{11}^h & \cdots & \Gamma_{1m}^h \\ \vdots & \ddots & \vdots \\ \Gamma_{m1}^h & \cdots & \Gamma_{mm}^h \end{bmatrix}, \tag{23}$$

repeatedly for $h = 1, 2, ..., m$. Given the transition probability matrix and according state space, Markov models can be directly formulated as graphically shown in Fig. 7. The state transition for existing three consequent states in the data history is represented in Fig. 7.a, where respective transition probabilities are shown in Fig. 7.b.

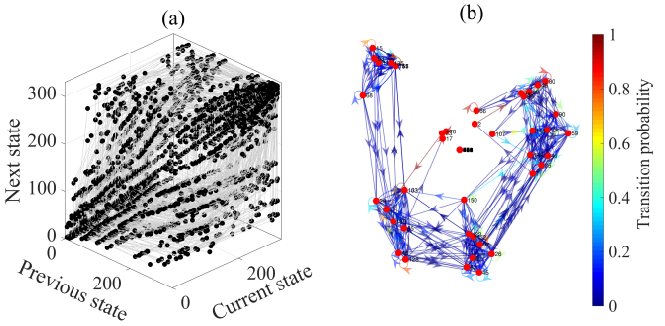

Figure 7: Transition patterns between vehicle states and according Markov chains in an exemplified grid-space constellation.

Considering an arbitrary initial state $S_k = s_i$ and preceding state $S_{k-1} = s_h$, a transition probability vector can be extracted as $[\Gamma_{i1}^h, \Gamma_{i2}^h, ..., \Gamma_{im}^h]$. In this contribution, only highest transition probabilities at each time step are considered for MPC, i.e. gradient weighting of stochastic Markov process is omitted. This prediction step is repeated for the whole moving horizon $k+N$.

3.3. Model predictive control

Provided situation-based solutions from offline optimization are only suitable to achieve local optimality at specific operating conditions. To approach global optimality, the full driving horizon can be broken down into smaller finite windows of time; in which online optimization can be performed. The longer these windows are, the closer the solution can get to global optimality [42]. That comes at the price of increased computational load and mitigated prediction accuracy for long horizons [13]. These two aspects are particularly addressed in the sequel.

The working principle of MPC illustrated in Fig. 8. Given a state prediction for N upcoming steps as

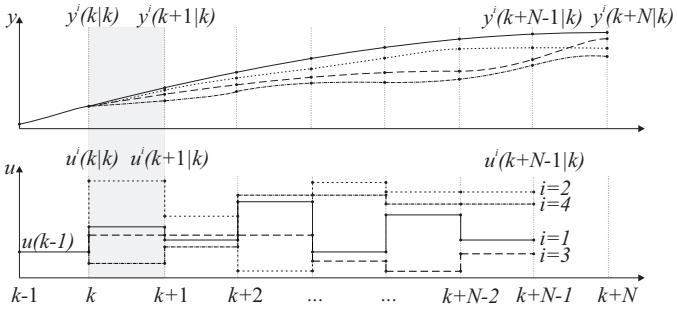

Figure 8: Different trajectories of predicted cost function $(y^i(k+1 \mid K), ..., y^i(k+N \mid K))$ for (N) look-ahead steps based on respective iterations (i) of the future control strategy $u^i(k), ..., u^i(k+N-1 \mid K)$.

$$\tilde{S}_{k+1:k+N|k-1,k} = \begin{bmatrix} \tilde{S}_{k+1} & \tilde{S}_{k+2} & ... & \tilde{S}_{k+N} \end{bmatrix}, \tag{24}$$

where the manipulated variable u^i at time instant k is defined as

$$u^i(k) = \begin{bmatrix} u^i(k \mid k) \\ \vdots \\ u^i(k+N-1 \mid k) \end{bmatrix}, \tag{25}$$

where i denotes current the iteration number of the initial variable $u^1(k)$ defined as

$$u^1(k+n-1 \mid k) = \begin{cases} \psi_i & \forall S_k = s_i \quad \& \quad n = 1 \\ \psi_j & \forall \tilde{S}_{k+n-1} = s_j \quad \& \quad n = 2,3,...,N. \end{cases} \tag{26}$$

As no set-point control is required, the estimated system output $\tilde{y}^i(k)$ according to certain manipulated variable $u^i(k)$ is formulated to directly represent the cost function, as similarly explained in Eqn. (17)-(19) with

$$J_{mpc} = \tilde{y}^i(u^i,x,t) = \begin{bmatrix} \tilde{y}_1^i(u^i,x,t) \\ \tilde{y}_2^i(u^i,x,t) \end{bmatrix} = \begin{bmatrix} \sum_{t=k}^{t=k+N} \tilde{m}_{eq}\Delta t \\ \alpha_1 \Delta SoC_b \mid_{t=k}^{t=k+N} + \alpha_2 \, \Delta SoC_{sc} \mid_{t=k}^{t=k+N} \end{bmatrix}, \tag{27}$$

where the optimization task is to minimize J_{mpc} over the look-ahead horizon subject to same constrains in Eqn. (20). These constraints address the plausibility of online optimization, i.e. sustaining the operating boundaries of individual powertrain components. Here, local optimality of J_{mpc} refers to minimal accumulated cost $\tilde{y}^*$ over N time steps according to an optimal manipulated vector $u^*(k \mid k)$. This control decision is applied for the recent time step k, the moving horizon is swept for one time step, and above-explained procedures are executed again for the new horizon.

Vehicle state prediction and output estimation at each iteration step are the main aspects determining the computational load in SB-MPC. Implementing the detailed powertrain model at each time steps for multiple iterations is computational adverse to the real-time application of SB-MPC. Therefore, a simplified powertrain model is essential to enable working on longer prediction horizons and carry out multiple iterations to approach global optimality. Operation of relevant powertrain components, i.e. fuel cell, battery, supercapacitor, and the inline DC/DC converters, can be simplified for each power source and respective converter linearly as a 3rd degree polynomial. The simplified models are tuned using curve fitting tools based on input/outputs data for each power source [55]. Simulation results of both original and simplified models for each power source including respective error are shown in Fig. 9. Simplified power flow dynamics in each component stimulates undamped behavior of the output. However, for optimization purpose over limited time horizons, this error is not significantly relevant as long as both results show similar behavior.

In Fig. 10, the significant reduction of elapsed time in the optimization process is shown, considering different look-ahead steps and number of iteration using the simplified powertrain model. The computational time is retained $\lessapprox 1$ ms, considering up to 15 steps ahead for optimization and 15 iterations per step using the simplified model (Fig. 10b), compared to $\gtrapprox$ 16 s required for 3 steps ahead and 3 iterations per step using the

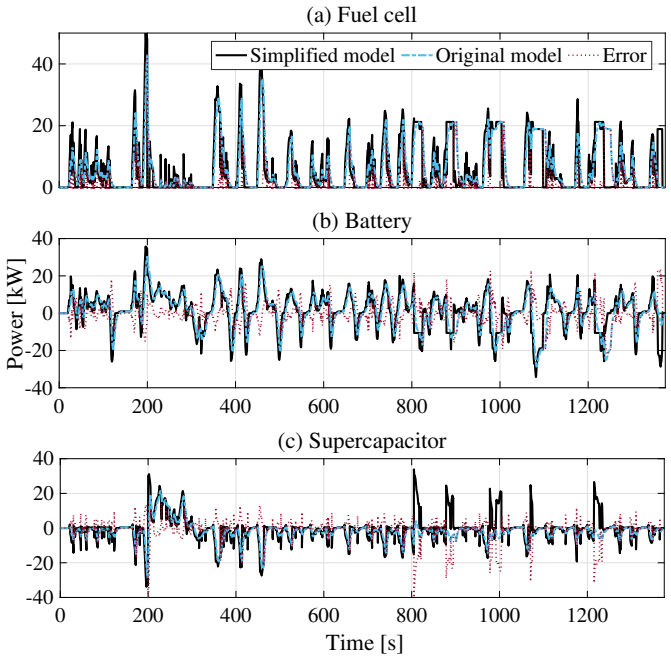

Figure 9: Dynamic behavior of the fuel cell, battery, and supercapacitor using the nonlinear and simplified HEV models over the NEDC driving cycle.

detailed powertrain model (Fig. 10a). Beside, the direct proportionality of computational time to the number of iterations is evidently larger than to the number of prediction steps in Fig. 10a. On the other side, in Fig. 10b, a quasi-homogeneous proportionality of the computational time to both prediction steps and the number of performed iterations is realized. The computational time in the latter case suits the real-time applicability for up to 10 input iterations for 10 steps ahead of state prediction.

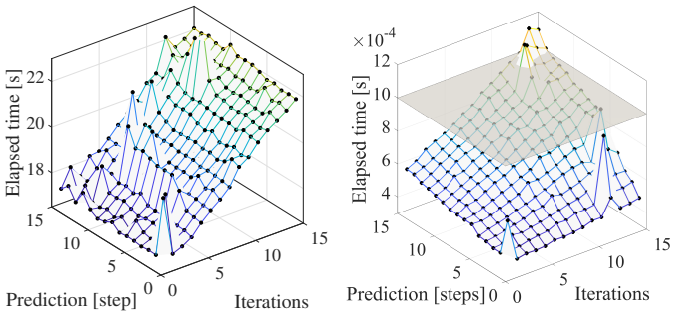

(a) Full detailed powertrain model (b) Simplified powertrain model

Figure 10: Elapsed time for optimization considering different look-ahead steps and iteration per steps in SB-MPC using detailed and simplified HEV models. Computational time is calculated for workbench with an AMD 4.01 GHz 8-core processor, 16 GB RAM operating a 64-Bit Windows professional. Real-time compatibility is verified for a dSPACE ds-4504 platform.

To sum up the working steps of SB-MPC, all above-explained steps are illustratively shown in Fig. 11. First, vehicle speed, calculated power demand, and the feed back signals of SoC_b and SoC_{sc} are linearly mapped to respective vehicle state in GS. Second, information about previous and current vehicle

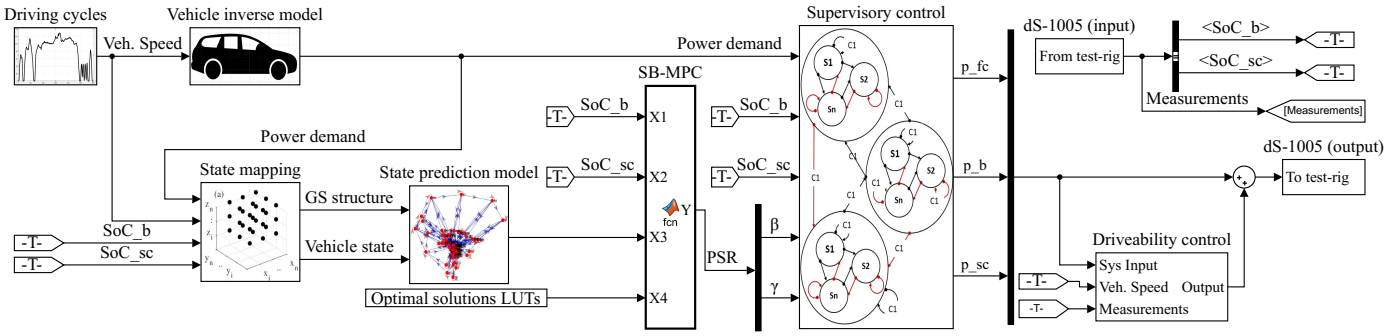

Figure 11: Implementation of SB-MPC as a Simulink model.

state are given to the Markov prediction model to provide the state prediction for upcoming horizon. Third, offline-optimized solutions to the predicted states are iterated using MPC algorithm to achieve near-global optimality of the cost function in Eqn. (27) over the considered look-ahead horizon. Fourth, optimized control vector u is verified through the supervisory control w.r.t. the operating boundaries of powertrain components. Finally, the control u is applied, the moving horizon is shifted one step ahead, and the whole procedures is repeated again.

4. Results analysis and discussion

Test procedures of developed SB-MPC comprise three steps: First, to verify the robustness of SB-MPC, it has been applied to a number of driving cycles including learned and non-learned ones, i.e. driving cycles which have been considered in offline optimization processes or not. Second, to obtain an insight to achieved results, a non-learned driving cycles during offline optimization is selected for further analysis, considering energy saving and operating efficiency. Third, a full-MPC solution is introduced, using the detailed powertrain model, to evaluate the impact of using simplified powertrain model on solution optimality of SB-MPC.

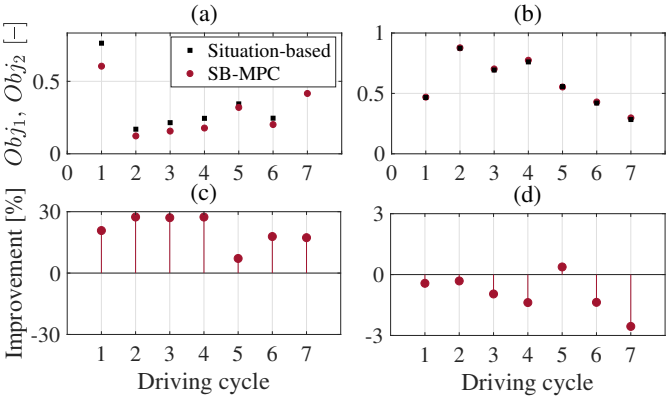

Figure 12: Cost function minimization results using situation-based RB method and SB-MPC for learned driving cycles (1-6) and a non-learned cycle (7): Top: objective functions obj_1 and obj_2 in figures (a) and (b) respectively, Bottom: according percentual improvement in figures (c) and (d).

In Fig. 12, the results of both objectives functions obj_1 and obj_1 using SB-MP and the conventional situation-based method are illustrated. Seven driving cycles are considered for the test, representing different urban and highway driving conditions [56]. An evident reduction of obj_1, pertaining fuel cell energy, is achieved using SB-MPC (Fig. 12.a.) This reduction in obj_1 corresponds to an improvement of 9–29 % compared to the conventional of situation-based solution (Fig. 12.c). Values of the contradictive objective obj_2, oppressing the depletion of SoC_b and SoC_{sc}, reveal 1–3 % increase in deployed power from the auxiliary sources using SB-MPC (Fig. 12.b and 12.d). Driving cycle modemIM-TUV is selected for further analysis of SB-MPC in the sequel, as it has not been considered for offline optimization (non-learned driving conditions).

Current consumption from each power source, using different control methods is shown in Fig. 13. Presented results reveal different power handling strategies to meet the control objective. For limited pre-knowledge of the future in SB-MPC, the power synergy ratio has changed dynamically over the moving horizon to count for inaccurate predictions of the system output. On the other, full-MPC has been more capable than other methods to perform scheduled charging/discharging cycles of the battery and supercapacitor to retain minimal fuel cell load.

To obtain an insight into the working mechanism of SB-MPC, the cost minimization process over the time horizon 50–63s is shown in Fig. 14. For each time step, 10 iterations of the manipulated variable u are performed to minimize estimated future cost for the upcoming time frame of 10s. Optimal control strategy for this horizon is applied, the moving horizon is shifted for one step, and the same optimization procedures are performed again. A significant reduction in the total energy consumption E_tot can be realized considering the proposed optimization strategy. Moreover, accurate prediction of upcoming vehicle states and future cost implies fast convergence to near-optimal solution as shown for this time-window, otherwise the control algorithm has to explore more value for u at each time step.

An important performance measure for power management methods is the ability to assign power synergy tasks to the battery and supercapacitor, reducing overall energy consumption, yet not depleting the onboard charge at the end of the driving cycle [57].The impact of assigned values for α_1 and α_2 in Eqn. (19) is revealed through the largest drop of $\Delta SoC_{sc} = 36.41$ %

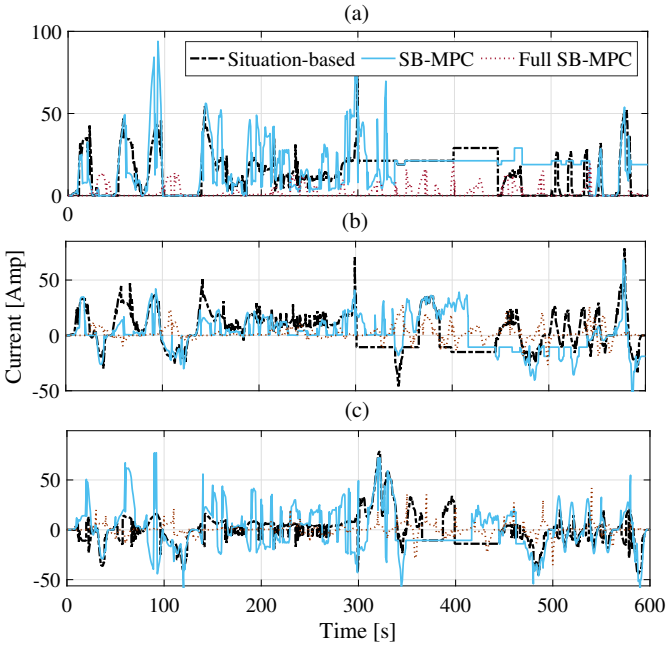

Figure 13: Current consumption of (a) fuel cell, (b) battery, and (c) supercapacitor over driving cycle modemIM-TUV.

using SB-MPC (Fig. 15.b). Final values of SoC_b are approximately similar for both SB-MPC and the classical situation-based method (Fig. 15.a). Minimal drop of both SoC_b and SoC_{sc} has been achieved using full-MPC as 17.9 and 2.02 % respectively.

For objective evaluation of the proposed method, detailed energy consumption facts for all methods are shown in Fig. 16. The online minimization of obj_1 and obj_2 considering more weighting for the fuel cell energy E_{fc}, results in more deployed energy from the battery ans supercapacitor E_b and E_{sc} to achieve balanced synergy ratio among all sources SB-MPC and full-MPC (16.a). The shifted loading of battery and supercapacitor is balanced using defined values for α_1 and α_2 to avoid components degradation.

The defined optimization criterion for J met and improvement in total energy minimization of 5 % up to 62 % using SB-MPC and full-MPC respectively (16.b). The outperformed optimality of SB-PMS puts forward the significance of accurate, yet simple plant model in the proposed method. However, the advantageous optimality of full-MPC is not realizable in real-time.

The overall powertrain efficiency can be mitigated by energy-saving strategies due to the necessity to operate the DC/DC converters within certain bounds. The significant reduction of fuel cell energy using full-MPC resulted in the largest drop of the fuel cell efficiency η_{fc}, considering DC/DC conversion efficiency. This effect is less for the battery and supercapacitor's efficiency η_b and η_{sc} (16.c).

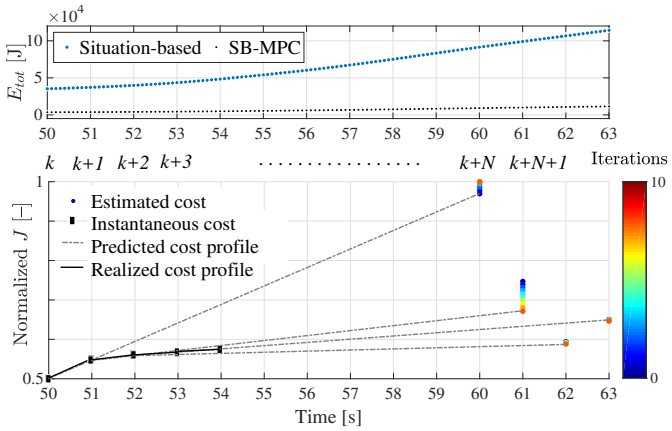

Figure 14: Cost minimization procedures over limited time horizon using SB-MPC

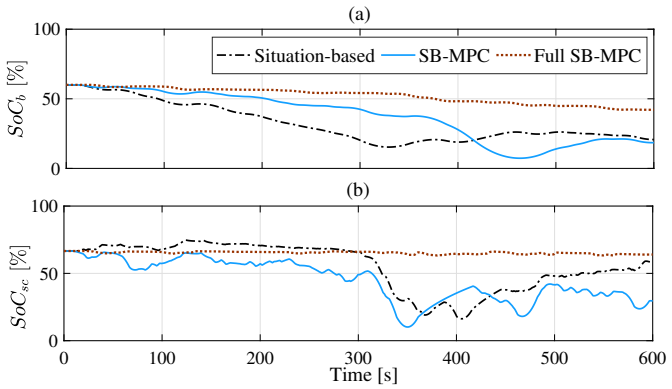

Figure 15: State-of-charge profiles for the battery and super capacitor SoC_b and SoC_{sc} using different power management methods.

5. Conclusion and outlook

In this paper, a novel power management method using situation-based MPC is presented. The proposed method implements pre-optimized solutions related to vehicle states for the online optimization using MPC. Vehicle states are defined in terms of optimized discrete levels for the variables: vehicle speed, power demand, speed dynamics, and battery- and supercapacitor state-of-charge. Optimization of control decisions related to each vehicle state is performed offline. State prediction models are developed based on transition statistics of vehicle states in a number of driving cycles. The online application comprises following steps: Anticipating upcoming vehicle states for limited time horizon, assigning optimized solutions to each predicted vehicle state, and iterating the local optimal solutions to achieve better optimality for the considered look-ahead window using MPC. The developed situation-based MPC (SB-MPC) is adapted to suit real-time application, in terms of prediction length and the number of iterations per step using a simplified powertrain model.

Online testing of SB-MPC is performed considering seven different driving cycles. Moreover, the proposed method is evaluated compared to the original situation-based PMS. Results analysis reveal the ability of SB-PMS to achieve robust

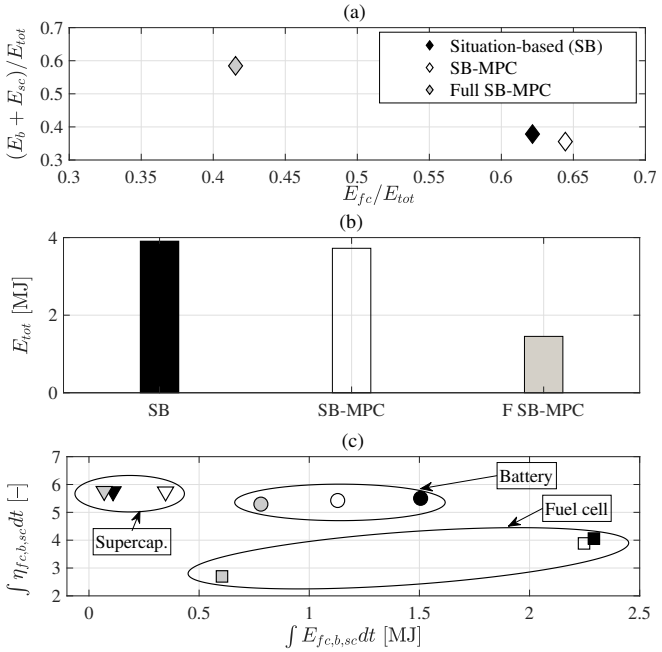

Figure 16: Energy saving results using different control strategies: (a) power synergy ration, (b) total consumed energy, (c) Depleted energy and electric efficiency for individual power sources.

improvement of defined cost function for all driving cycles. The evaluation regarding energy consumption results shows the ability of SB-PMS to realize balanced power split among the fuel cell, battery, and supercapacitor and to achieve up to 5 % reduction in total energy. However, considering detailed vehicle model in the optimization process, 62 % reduction of total energy in offline simulation can be achieved. These results put forward the significance of accurate plant model to define optimal power management strategies using SB-MPC. Next steps of this work includes the improvement of an accurate, yet real-time-applicable plant models for SB-MPC.

References

[1] J. Du, M. Ouyang, J. Chen, Prospects for chinese electric vehicle technologies in 2016–2020: Ambition and rationality, Energy 120 (2017) 584–596 (Feb. 2017). doi:10.1016/j.energy.2016.11.114.

[2] S. F. Tie, C. W. Tan, A review of energy sources and energy management system in electric vehicles, Renewable and Sustainable Energy Reviews 20 (2013) 82–102 (Apr. 2013). doi:10.1016/j.rser.2012.11.077.

[3] S. Habib, M. Kamran, U. Rashid, Impact analysis of vehicle-to-grid technology and charging strategies of electric vehicles on distribution networks – a review, Journal of Power Sources 277 (2015) 205–214 (Mar. 2015). doi:10.1016/j.jpowsour.2014.12.020.

[4] H. Fathabadi, Novel fuel cell/battery/supercapacitor hybrid power source for fuel cell hybrid electric vehicles, Energy 143 (2018) 467–477 (Jan. 2018). doi:10.1016/j.energy.2017.10.107.

[5] M. Ehsani, Y. Gao, S. Longo, K. Ebrahimi, Modern Electric, Hybrid Electric, and Fuel Cell Vehicles, Third Edition, Boca Raton: CRC Press, 2018 (Feb. 2018). doi:10.1201/9780429504884.

[6] M. Sabri, K. Danapalasingam, M. Rahmat, A review on hybrid electric vehicles architecture and energy management strategies, Renewable and Sustainable Energy Reviews 53 (2016) 1433–1442 (2016).

[7] Y. Cui, Z. Geng, Q. Zhu, Y. Han, Review: Multi-objective optimization methods and application in energy saving, Energy 125 (2017) 681–704 (Apr. 2017). doi:10.1016/j.energy.2017.02.174.

[8] E. Silvas, T. Hofman, N. Murgovski, L. F. P. Etman, M. Steinbuch, Review of optimization strategies for system-level design in hybrid electric vehicles, IEEE Transactions on Vehicular Technology 66 (1) (2017) 57–70 (Jan. 2017). doi:10.1109/TVT.2016.2547897.

[9] A. M. Ali, D. Söffker, Towards optimal power management of hybrid electric vehicles in real-time: A review on methods, challenges, and state-of-the-art solutions, Energies 11 (3) (2018). doi:10.3390/en11030476.

[10] R. Langari, J.-S. Won, Intelligent energy management agent for a parallel hybrid vehicle-part i: system architecture and design of the driving situation identification process, IEEE Transactions on Vehicular Technology 54 (3) (2005) 925–934 (May 2005). doi:10.1109/TVT.2005.844685.

[11] Y. Zhou, A. Ravey, M.-C. Péra, A survey on driving prediction techniques for predictive energy management of plug-in hybrid electric vehicles, Journal of Power Sources 412 (2019) 480–495 (Feb. 2019). doi:10.1016/j.jpowsour.2018.11.085.

[12] Y. Huang, H. Wang, A. Khajepour, H. He, J. Ji, Model predictive control power management strategies for HEVs: A review, Journal of Power Sources 341 (2017) 91–106 (Feb. 2017). doi:10.1016/j.jpowsour.2016.11.106.

[13] S. Kutter, B. Bäker, Predictive online control for hybrids: Resolving the conflict between global optimality, robustness and real-time capability, in: 2010 IEEE Vehicle Power and Propulsion Conference, IEEE, 2010 (Sep. 2010). doi:10.1109/vppc.2010.5729231.

[14] J. Soon-il, J. Sung-tae, P. Yeong-il, L. Jang-moo, Multi-mode driving control of a parallel hybrid electric vehicle using driving pattern recognition, Journal of Dynamic Systems, Measurement, and Control 124 (1) (2000) 141–149 (2000). doi:10.1115/1.1434264.

[15] H. Hongwen, G. Jinquan, P. Jiankun, T. Huachun, S. Chao, Real-time global driving cycle construction and the application to economy driving pro system in plug-in hybrid electric vehicles, Energy 152 (2018) 95–107 (Jun. 2018). doi:10.1016/j.energy.2018.03.061.

[16] S. Zhang, R. Xiong, Adaptive energy management of a plug-in hybrid electric vehicle based on driving pattern recognition and dynamic programming, Applied Energy 155 (2015) 68–78 (Oct. 2015). doi:10.1016/j.apenergy.2015.06.003.

[17] Y. Zou, Z. Kong, T. Liu, D. Liu, A real-time markov chain driver model for tracked vehicles and its validation: Its adaptability via stochastic dynamic programming, IEEE Transactions on Vehicular Technology 66 (5) (2017) 3571–3582 (May 2017). doi:10.1109/TVT.2016.2605449.

[18] C. M. Martinez, M. Heucke, F. Wang, B. Gao, D. Cao, Driving style recognition for intelligent vehicle control and advanced driver assistance: A survey, IEEE Transactions on Intelligent Transportation Systems 19 (3) (2018) 666–676 (Mar. 2018). doi:10.1109/TITS.2017.2706978.

[19] J. Nilsson, M. Brännström, E. Coelingh, J. Fredriksson, Lane change maneuvers for automated vehicles, IEEE Transactions on Intelligent Transportation Systems 18 (5) (2017) 1087–1096 (May 2017). doi:10.1109/TITS.2016.2597966.

[20] M. Montazeri-Gh, Z. Pourbafarani, Near-optimal soc trajectory for traffic-based adaptive PHEV control strategy, IEEE Transactions on Vehicular Technology 66 (11) (2017) 9753–9760 (Nov. 2017). doi:10.1109/TVT.2017.2757604.

[21] Y. Han, Q. Li, T. Wang, W. Chen, L. Ma, Multisource coordination energy management strategy based on soc consensus for a pemfcbatterysupercapacitor hybrid tramway, IEEE Transactions on Vehicular Technology 67 (1) (2018) 296–305 (Jan.. 2018). doi:10.1109/TVT.2017.2747135.

[22] H. Li, A. Ravey, A. N'Diaye, A. Djerdir, A novel equivalent consumption minimization strategy for hybrid electric vehicle powered by fuel cell, battery and supercapacitor, Journal of Power Sources 395 (2018) 262 270 (2018). doi:https://doi.org/10.1016/j.jpowsour.2018.05.078.

[23] Z. Chen, Y. Wu, N. Guo, J. Shen, R. Xiao, Energy management for plug-in hybrid electric vehicles based on quadratic programming with optimized engine on-off sequence, in: IECON 2017 - 43rd Annual Conference of the IEEE Industrial Electronics Society, IEEE, 2017 (Oct. 2017). doi:10.1109/iecon.2017.8217248.

[24] M. Li, H. He, M. Yan, J. Peng, Variable horizon MPC for energy management on dual planetary gear hybrid electric vehicle, Energy Procedia 152 (2018) 636 642, cleaner Energy for Cleaner Cities (2018). doi:https://doi.org/10.1016/j.egypro.2018.09.223.

[25] S. Kelouwani, N. Henao, K. Agbossou, Y. Dube, L. Boulon, Two-layer energy-management architecture for a fuel cell HEV using road trip information, IEEE Transactions on Vehicular Technology 61 (9) (2012) 3851–

3864 (Nov. 2012). doi:10.1109/TVT.2012.2214411.

[26] L. Guo, B. Gao, Y. Gao, H. Chen, Optimal energy management for HEVs in eco-driving applications using bi-level MPC, IEEE Transactions on Intelligent Transportation Systems 18 (8) (2017) 2153–2162 (Aug. 2017). doi:10.1109/TITS.2016.2634019.

[27] H. He, J. Guo, C. Sun, Road grade prediction for predictive energy management in hybrid electric vehicles, Energy Procedia 105 (2017) 2438–2444 (May 2017). doi:10.1016/j.egypro.2017.03.700.

[28] Z. Chen, C. C. Mi, J. Xu, X. Gong, C. You, Energy management for a power-split plug-in hybrid electric vehicle based on dynamic programming and neural networks, IEEE Transactions on Vehicular Technology 63 (4) (2014) 1567–1580 (May 2014). doi:10.1109/TVT.2013.2287102.

[29] X. Zeng, J. Wang, A parallel hybrid electric vehicle energy management strategy using stochastic model predictive control with road grade preview, IEEE Transactions on Control Systems Technology 23 (6) (2015) 2416–2423 (Nov. 2015). doi:10.1109/TCST.2015.2409235.

[30] B. Geng, J. K. Mills, D. Sun, Two-stage energy management control of fuel cell plug-in hybrid electric vehicles considering fuel cell longevity, IEEE Transactions on Vehicular Technology 61 (2) (2012) 498–508 (Feb. 2012). doi:10.1109/TVT.2011.2177483.

[31] C. Zhang, A. Vahidi, P. Pisu, X. Li, K. Tennant, Role of terrain preview in energy management of hybrid electric vehicles, IEEE Transactions on Vehicular Technology 59 (3) (2010) 1139–1147 (Mar. 2010). doi:10.1109/TVT.2009.2038707.

[32] D. Zhou, A. Al-Durra, F. Gao, A. Ravey, I. Matraji, M. G. Simes, Online energy management strategy of fuel cell hybrid electric vehicles based on data fusion approach, Journal of Power Sources 366 (2017) 278 – 291 (2017). doi:10.1016/j.jpowsour.2017.08.107.

[33] R. Zhang, J. Tao, H. Zhou, Fuzzy optimal energy management for fuel cell and supercapacitor systems using neural network based driving pattern recognition, IEEE Transactions on Fuzzy Systems (2018) 1 (2018). doi:10.1109/TFUZZ.2018.2856086.

[34] S. Xie, X. Hu, T. Liu, S. Qi, K. Lang, H. Li, Predictive vehicle-following power management for plug-in hybrid electric vehicles, Energy 166 (2019) 701–714 (Jan. 2019). doi:10.1016/j.energy.2018.10.129.

[35] H. Chen, F. Allgöwer, A quasi-infinite horizon nonlinear model predictive control scheme with guaranteed stability., Automatica 34 (10) (1998) 1205–1217 (Oct. 1998). doi:10.1016/s0005-1098(98)00073-9.

[36] P. Zhang, F. Yan, C. Du, A comprehensive analysis of energy management strategies for hybrid electric vehicles based on bibliometrics, Renewable and Sustainable Energy Reviews 48 (2015) 88–104 (Aug. 2015). doi:10.1016/j.rser.2015.03.093.

[37] S. Zhang, R. Xiong, F. Sun, Model predictive control for power management in a plug-in hybrid electric vehicle with a hybrid energy storage system, Applied Energy 185 (2017) 1654–1662 (Jan. 2017). doi:10.1016/j.apenergy.2015.12.035.

[38] M. Lorenzen, M. Cannon, F. Allgöwer, Robust MPC with recursive model update, Automatica 103 (2019) 461–471 (May 2019). doi:10.1016/j.automatica.2019.02.023.

[39] M. Ławryńczuk, Computationally Efficient Model Predictive Control Algorithms, Springer International Publishing, 2014 (2014). doi:10.1007/978-3-319-04229-9.

[40] L. Li, S. You, C. Yang, B. Yan, J. Song, Z. Chen, Driving-behavior-aware stochastic model predictive control for plug-in hybrid electric buses, Applied Energy 162 (2016) 868–879 (Jan. 2016). doi:10.1016/j.apenergy.2015.10.152.

[41] S. D. Cairano, D. Bernardini, A. Bemporad, I. V. Kolmanovsky, Stochastic MPC with learning for driver-predictive vehicle control and its application to HEV energy management, IEEE Transactions on Control Systems Technology 22 (3) (2014) 1018–1031 (May 2014). doi:10.1109/tcst.2013.2272179.

[42] T. Li, H. Liu, D. Ding, Predictive energy management of fuel cell supercapacitor hybrid construction equipment, Energy 149 (2018) 718–729 (Apr. 2018). doi:10.1016/j.energy.2018.02.101.

[43] M. Esfandyari, V. Esfahanian, M. H. Yazdi, H. Nehzati, O. Shekoofa, A new approach to consider the influence of aging state on lithium-ion battery state of power estimation for hybrid electric vehicle, Energy 176 (2019) 505–520 (Jun. 2019). doi:10.1016/j.energy.2019.03.176.

[44] F. Yan, J. Wang, K. Huang, Hybrid electric vehicle model predictive control torque-split strategy incorporating engine transient characteristics, IEEE Transactions on Vehicular Technology 61 (6) (2012) 2458–2467 (Jul. 2012). doi:10.1109/tvt.2012.2197767.

[45] G. Ripaccioli, A. Bemporad, F. Assadian, C. Dextreit, S. D. Cairano, I. V. Kolmanovsky, Hybrid modeling, identification, and predictive control: An application to hybrid electric vehicle energy management, in: Hybrid Systems: Computation and Control, Springer Berlin Heidelberg, 2009, pp. 321–335 (2009). doi:10.1007/978.3.642.00602.9.23.

[46] M. Back, M. Simons, F. Kirschaum, V. Krebs, Predictive control of drivetrains, IFAC Proceedings Volumes 35 (1) (2002) 241–246 (2002). doi:10.3182/20020721-6-es-1901.01508.

[47] M. Koot, J. Kessels, B. deJager, W. Heemels, P. vandenBosch, M. Steinbuch, Energy management strategies for vehicular electric power systems, IEEE Transactions on Vehicular Technology 54 (3) (2005) 771–782 (May 2005). doi:10.1109/tvt.2005.847211.

[48] G. Jinquan, H. Hongwen, P. Jiankun, Z. Nana, A novel MPC-based adaptive energy management strategy in plug-in hybrid electric vehicles, Energy 175 (2019) 378–392 (May 2019). doi:10.1016/j.energy.2019.03.083.

[49] J. Kuhn, C. Reinl, O. von Stryk, Predictive control for multi-robot observation of multiple moving targets based on discrete-continuous linear models, IFAC Proceedings Volumes 44 (1) (2011) 257–262 (Jan. 2011). doi:10.3182/20110828-6-it-1002.00274.

[50] S. Xie, X. Hu, S. Qi, X. Tang, K. Lang, Z. Xin, J. Brighton, Model predictive energy management for plug-in hybrid electric vehicles considering optimal battery depth of discharge, Energy 173 (2019) 667–678 (Apr. 2019). doi:10.1016/j.energy.2019.02.074.

[51] M. Özbek, S. Wang, M. Marx, D. Söffker, Modeling and control of a PEM fuel cell system: A practical study based on experimental defined component behavior, Journal of Process Control 23 (3) (2013) 282–293 (Mar. 2013). doi:10.1016/j.jprocont.2012.11.009.

[52] A. M. Ali, R. Shivapurkar, D. Söffker, Development and improvement of a situation-based power management method for multi-source electric vehicles, in: 2018 IEEE Vehicle Power and Propulsion Conference (VPPC), IEEE, 2018 (Aug. 2018). doi:10.1109/vppc.2018.8604988.

[53] K. Deb, A. Pratap, S. Agarwal, T. Meyarivan, A fast and elitist multiobjective genetic algorithm: NSGA-II, IEEE Transactions on Evolutionary Computation 6 (2) (2002) 182–197 (Apr. 2002). doi:10.1109/4235.996017.

[54] S. Lin, NGPM – A NSGA-II Program in Matlab v1.4 (2011). URL `https://de.mathworks.com /matlabcentral/fileexchange /31166-ngpm-a-nsga-ii-program- in-matlab-v1-4`

[55] A. M. Ali, D. Söffker, Realtime application of progressive optimal search and adaptive dynamic programming in multi-source HEVs, in: Volume 2: ASME DSCC 2017 - Dynamic Systems and Control Conference, ASME, 2017, doi: 10.1115/dscc2017-5081 (Oct. 2017).

[56] S. Caux, Y. Gaoua, P. Lopez, A combinatorial optimisation approach to energy management strategy for a hybrid fuel cell vehicle, Energy 133 (2017) 219–230 (Aug. 2017). doi:10.1016/j.energy.2017.05.109.

[57] S. Onori, L. Serrao, G. Rizzoni, Hybrid Electric Vehicles, Springer London, 2016 (2016). doi:10.1007/978-1-4471-6781-5.